OCEANOLOGICA ACTA · VOL. 24 – No. 2

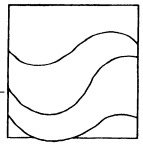

Variability and seasonality of physical and biological fields at the Great Meteor Tablemount (subtropical NE Atlantic)

Beatriz MOURIÑO[a]*, Emilio FERNÁNDEZ[a], Pablo SERRET[a], Derek HARBOUR[b], Bablu SINHA[c], Robin PINGREE[d]

[a] Departamento de Ecoloxía e Bioloxía Animal, Universidade de Vigo, Campus Lagoas-Marcosende, 36200 Vigo, Spain

[b] SAHFOS, The Hoe, Plymouth, PL1 3 BN, UK

[c] Southampton Oceanography Centre, Southampton, SO14 3ZH, UK

[d] The Laboratory, MBA Citadel Hill, Plymouth PL1 2PB, UK

Received 21 August 2000; revised 20 November 2000; accepted 21 November 2000

Abstract − Five oceanographic surveys were conducted at the Great Meteor Tablemount (subtropical NE Atlantic; 30.0ºN, 28.5ºW) throughout the 1992–1999 period to investigate temporal variability in the relationship between the physical structure of the water column associated with the seamount and phytoplankton biomass and/or production rates. Local increases in chlorophyll *a*, enhanced carbon incorporation rates and changes in phytoplankton species composition were associated with the seamount. These effects were subjected to a large degree of temporal and spatial variability both at seasonal and shorter time scales. © 2001 Ifremer/CNRS/IRD/Éditions scientifiques et médicales Elsevier SAS

physical variability / phytoplankton / primary production / seamount / subtropical Atlantic

Résumé − Variabilité et caractéristiques saisonnières des champs physique et biologique du Mont sous-marin Great Meteor (Atlantique subtropical NE). Entre 1992 et 1999 cinq campagnes de recherche océanographique ont été réalisées (30,0ºN, 28,5ºO), pour étudier la variabilité temporelle du rapport entre la structure physique de la colonne d'eau associée aux abords du mont sous-marin d'une part, et la biomasse et les taux de production phytoplanctonique d'autre part. On observe une élévation locale de la teneur en chlorophylle *a* près du mont sous-marin ainsi que des taux élevés de production primaire et des changements de la composition spécifique du phytoplancton. Ces effets connaissent une variabilité spatiale et temporelle élevée, aussi bien à courte échelle de temps qu'à l'échelle saisonnière. © 2001 Ifremer/CNRS/IRD/Éditions scientifiques et médicales Elsevier SAS

variabilité physique / phytoplancton / production primaire / mont sous-marin / Atlantique subtropical

1. INTRODUCTION

The interaction of seamounts with ocean currents is known to generate variability in the physical flow field at different scales. At large spatial scales, seamounts can induce a deflection of current (Roden and Taft, 1985; Vastano et al., 1985). At shorter scales, reflected internal gravity waves (Eriksen, 1991; Eriksen et al., 1982), seamount-trapped topographic waves (Brink, 1990; Codiga, 1997a, b; Codiga and Eriksen, 1997), reflection, amplification and distortion of internal waves (Eriksen,

**Correspondence and reprints: fax*: +34 986 812 556.
E-mail address: beame@uvigo.es (B. MOURIÑO).

© 2001 Ifremer/CNRS/IRD/Éditions scientifiques et médicales Elsevier SAS. Tous droits réservés
S0399178400011385/FLA

1982, 1985, 1991; Kaneko et al., 1986) and amplification of diurnal and semidiurnal tides (Genin et al., 1989; Kunze and Toole, 1997; Noble and Mullineaux, 1989) have been reported. Seamounts have also found to be sites of amplified turbulent mixing (Kunze and Toole, 1997; Lueck and Mudge, 1997; Navatov and Ozmidov, 1988). Uplifting of isotherms and formation and shedding of mesoscale anticyclonic and cyclonic eddies, which can alter the flow patterns for significant distances downstream from the seamount, have been described in several studies (Meincke, 1971; Owens and Hogg; 1980; Roden, 1991; Vastano and Warren, 1976). Some barotropic flow patterns over and around banks have been given by Pingree and Maddock (1985).

A considerable body of knowledge on the biology of seamounts has been built up over the last two decades (reviewed by Rogers, 1994). Sharp differences in diverse biological variables have been frequently observed between seamounts and adjacent water, both in the pelagic and benthic domains. Investigations on the relationship between seamounts and phytoplankton biomass distribution and/or primary production are scarce and somewhat contradictory (references in Rogers, 1994). It has been hypothesised that increases in primary production rates over seamounts are related to high abundance of demersal and pelagic fishes (Uchida and Tagami, 1984). However, same investigations failed to demonstrate persistent high chlorophyll *a* patches over seamounts (Pelaez and McGowan, 1986).

The lack of agreement among the different observations is likely to stem from changes in the physical field at different temporal scales. Genin and Boehlert (1985) pointed out the existence of sharp differences in the physical conditions and associated phytoplankton response at Minami–Kasuga.

Seamount over a 17 days period. To our knowledge, investigations of the same nature focused on changing physical and biological characteristics over seasonal time scales have not been undertaken despite being needed for a better understanding of the dynamics of these systems.

With this aim, we have been carrying out research at the Great Meteor Tablemount (GMT) during the last eight years to investigate temporal variability in relationship to the physical structure associated with the seamount and the distribution of phytoplankton biomass and production.

2. METHODS

2.1. Cruises

Great Meteor Tablemount located at 30.0ºN, 28.5ºW rises from depths greater than 4500 m to just less than 300 m, with a flat top plateau of approximately 50 km in diameter (*figure 1*). GMT has been visited five times since 1992 as part of different oceanographic cruises. In March 1992, we first sampled GMT on board *Charles Darwin*, cruise CD66, when thirteen stations were conducted along the 30ºN parallel from 29.1ºW to 28.0ºW. GMT was visited again in December 1993 during cruise CD83 also on board *Charles Darwin*, when three stations were sampled over and around the seamount. GMT was also studied in October 1995 (CD97) and in August 1998 (Azores I, A1), on board *Charles Darwin* and *Hespérides*, respectively. In October 1995 (CD97), two stations were conducted and studied, one on GMT and one in deep-sea waters; in August 1998 (Azores I), there was only one station on GMT. Finally, an intensive conductivity temperature depth (CTD) survey was carried out in April 1999 on board *Hespérides*, as part of cruise Azores II (A2).

2.2. Moorings

Five short-term moorings were deployed on CD66 to investigate the tidal and inertial climate associated with GMT (*table I*). In all, eleven current meters were placed between the near surface (28 m) and 530 m (12 m off the sea floor) on four rigs A, B, C, D. In addition to the four current meter moorings, a self-contained bottom mounted acoustic doppler current profiler (ADCP) was deployed at L (rig L) near a central position within the 300 m depth contour for a period of four days (*figure 2a*).

2.3. Argos buoys

Five Argos were deployed in the vicinity of GMT on CD66. Four buoys were drogued at 200 m depth; three were released from the centre of GMT and one (3348) was placed on the western flank. A further Argos buoy (8336) was fitted with two current meters, a 200 m thermistor chain (with eleven thermistors) and a trans-

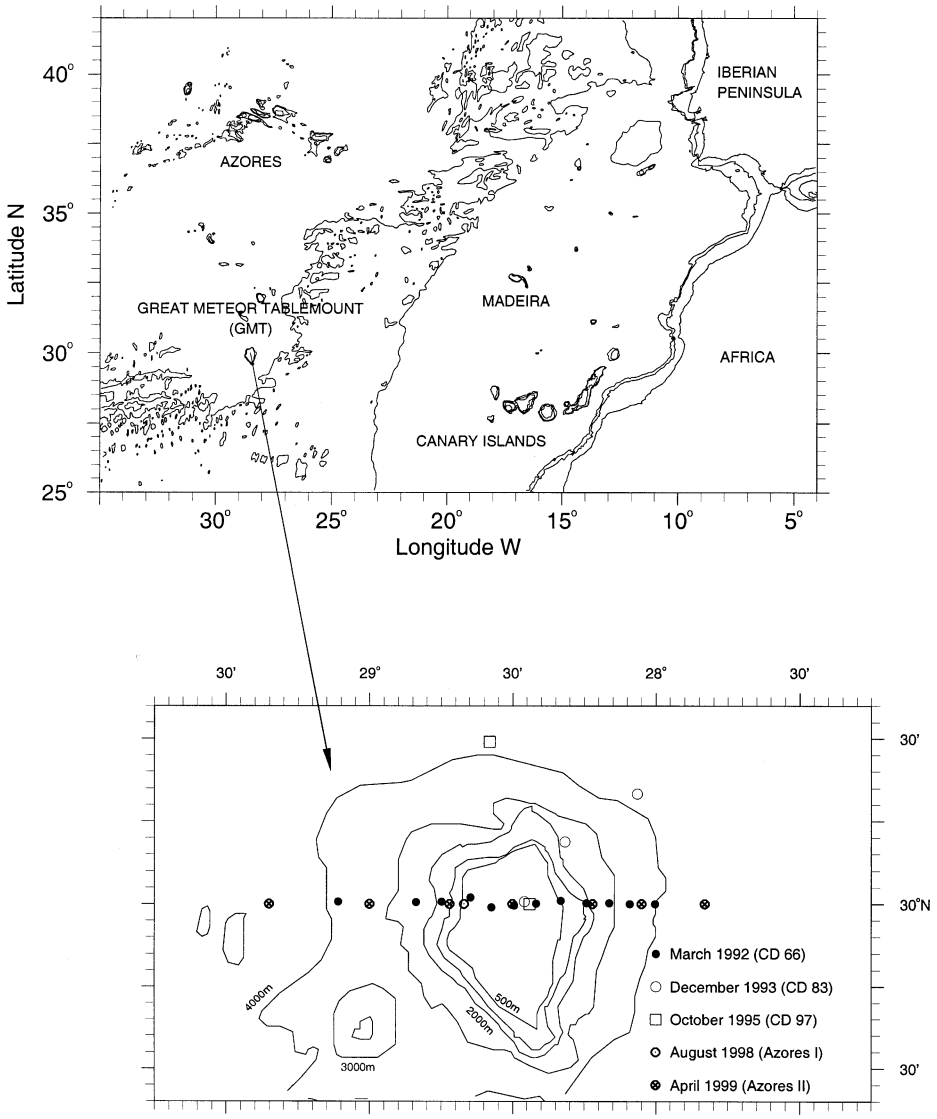

Figure 1. Location of Great Meteor Tablemount and stations visited during cruise CD66 (March 1992), CD83 (December 1993), CD97 (October 1995), Azores I (August 1998) and Azores II (April 1999).

missometer and released from the centre of the bank, near rig L. The chain extended from 11 to 211 m depth. This buoy was recovered after four days when the ship left the region. One Argos buoy (3898) was deployed from the centre of the bank on CD83 and one buoy (3345) was released on CD97; these buoys were also drogued at 200 m depth.

2.4. Hydrographic sampling

CTD profiles were conducted with Neil Brown Mark III probes attached to a rosette equipped with Niskin bottles. For the *Charles Darwin* cruises, the CTD was fitted with a SeaTech transmissometer, an Aquatracka for chlorophyll *a* fluorescence, and an oxygen probe. CTD tem-

Table I. Summary of characteristics of current meter moorings and self-contained ADCP.

Mooring, Latitude, Longitude	Water depth (m)	Current meter	Current depth (m)	Start date	Record length (days)	Sampling interval (min)	Mean temperature from yearday 68–70 (1992) (ºC)
A	311	7401	50	7.3.92	3.6	5	18.96
30º07.26		7517	148	7.3.92	3.6	5	18.02
28º29.84		420	299	7.3.92	3.6	5	15.47
B	435	7765	71	–	–	–	–
29º58.15		5204	222	8.3.92	3.7	5	16.89
28º19.84		1260	423	8.3.92	3.7	5	14.07
C	288	421	28	8.3.92	2.6	5	19.35
29º54.19		1259	126	8.3.92	2.6	5	18.43
28º33.99							
D	542	8010	58	8.3.92	2.6	5	19.36
29º49.17		6372	259	8.3.92	2.6	5	16.20
28º39.50		7943	530	8.3.92	2.6	5	12.42
L		ADCP					
30º00.26	306	349	306	7.3.92	4.0	15	15.4
28º27.35							

perature and salinity sensors were calibrated using digital reversing thermometers and water samples drawn for salinity determinations. Expendable bathythermographs (XBTs) were also used extensively throughout the Azores II cruise to obtain fine scale temperature distributions.

Samples were collected on each CTD cast to determinate of dissolved inorganic nutrients, chlorophyll *a*, phytoplankton species composition and primary production rates. Nitrate concentration was measured by continuous flow analysis following the methods described in Grasshoff et al. (1983) (CD83, CD97). Samples were also drawn for oxygen calibrations. Chlorophyll *a* was measured by fluorimetry after filtration of seawater onto different types of filters (GF/F on CD66 and CD97, and 0.2 µm polycarbonate filters on the other cruises), after extraction with acetone 90% overnight. In addition, size-fractionated (0.2 and > 2 µm) chlorophyll *a* was determined in CD83, Azores I and Azores II cruises. Chemically determined chlorophyll *a* values were used to calibrate the fluorometer on the CTD. Samples for microplankton identification and counting were collected on CD66, CD83 and Azores II cruises and preserved in lugol's iodine solution and formaldehyde. Samples were counted and the biomass of the different species estimated as in Holligan et al. (1984).

Primary production rates were determined in all cruises over a 7 to 11 h period, except for CD97 where incubations lasted 24 h period. CD97 data were not used in this study as they were not comparable due to their different incubation time. Triplicate 70 mL acid-cleaned polycarbonate bottles were filled with water from five or six depths corresponding to optical depths ranging from 100 to 0.1% of surface irradiance levels. Bottles were inoculated with 486–540 kBq (13.5–15 µCi) $NaH14CO_3$ and immediately placed in an on-deck incubator cooled by surface waters. Samples were incubated at irradiances corresponding approximately to those experienced by the cells at the sampling depths. After the incubation period, samples were filtered at very low vacuum pressure (< 50 mm Hg) through the same type of filters mentioned for chlorophyll *a* determinations. Filters were decontaminated by exposing them to fumes of concentrated HCl for 12 h. Radioactivity was determined by liquid scintillation counting either ashore (CD66, CD83, Azores I) or on board (Azores II). Quenching corrections were performed using an external standard. The variation coefficient for replicate primary production determinations was always lower than 15%.

3. RESULTS

3.1. Drogued buoy tracks and moorings records

In March 1992 (CD66), two of the drogued Argos buoys showed some trapping of the flow by the seamount.

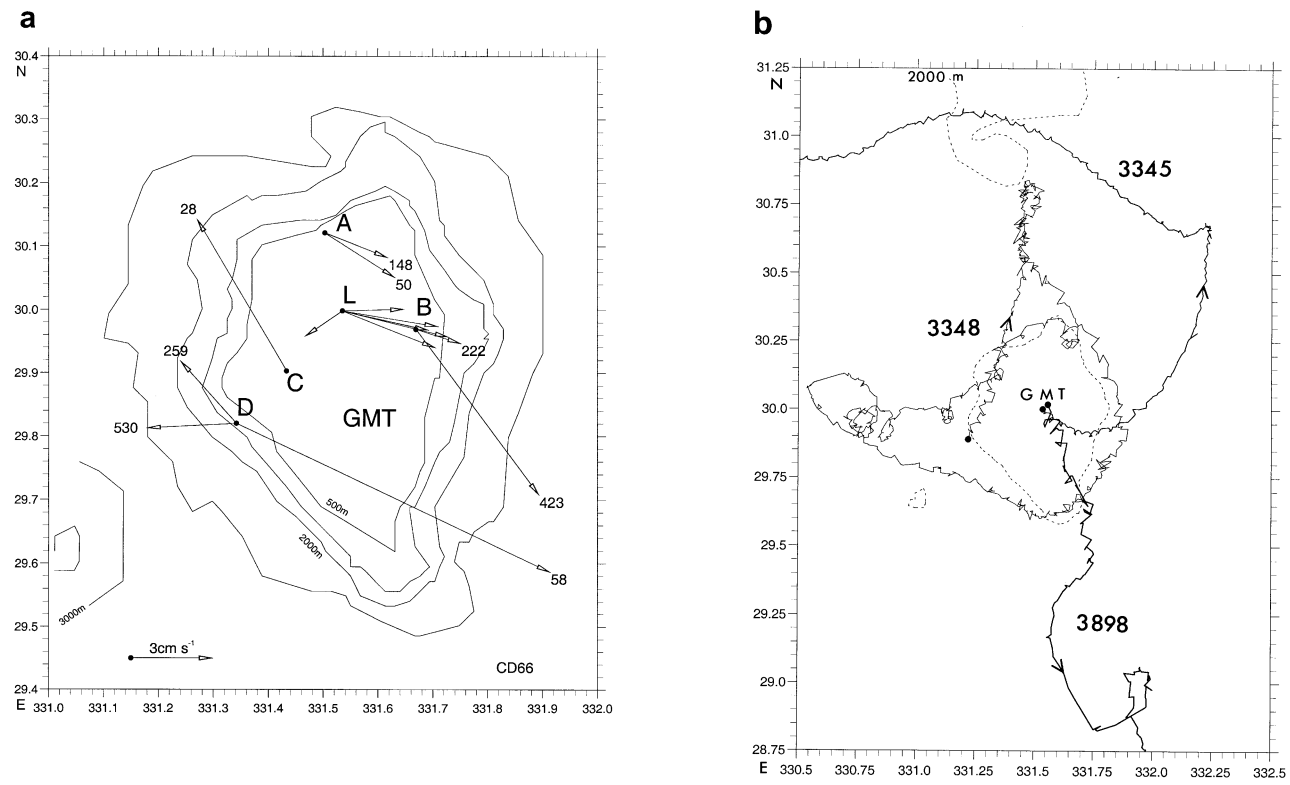

Figure 2. a. Great Meteor Tablemount and moorings positions of rigs A, B, C, D and L deployed in March 1992 (CD66). Arrows show short term residual current. Numbers near arrow heads are the depths (in meters) of the current meters (see . L is a bottom mounted self-contained ADCP and current vectors are plotted every 32 m from 288 m to 128 m depth (see for further details). A 3 cm s–1 scale is shown at bottom left. Water depth contours are 3000 m, 2000 m, 1000 m and 500 m. **b.** Raw data tracks of buoys 3348 (CD66), 3898 (CD83) and 3345 (CD97). The number of days of track shown are 98 (070–168 yearday, 1992), 42 (358–035 yearday, 1993/1994) and 39 (289–328 yearday, 1995), respectively. The drogues are at 200 m depth. The start position is shown with a dot; 2000 m water depth contour dashed.

Buoy 3348 followed an anticyclonic motion, although making excursions of the order of 100 km from the seamount centre (Pingree, 1997). In December 1993 (CD83) and October 1995 (CD97), the Argos buoys did not show trapping of water by the seamount (*figure 2b*). With the data obtained from the buoy tracks, it is possible to estimate a time scale or residence time for the water over the seamount. There were nine occasions when the buoys either crossed the seamount from the 2000 m bathymetric contour or went from the centre of the seamount to the 2000 m contour. Seven of these were independent and gave a mean of 21 days to cross the bank. This can be interpreted as a mean displacement velocity of 2.9 km d^{-1} across the bank. The three buoys deployed near the centre of the bank (300 m depth) gave a diffusive scale. About 6 days after deployment, the buoys were near the 2000 m contour and their root mean squared separation was 4 km, giving a mean diffusive separation rate of 0.7 km d^{-1}. Although more observations would be desirable, the results show that for the period of the observations the advective scale exceeds the diffusive scale and so water or properties are flushed off the bank rather than removed by local eddy diffusion from an anticyclonic vortex.

Short records (4 days) from four current meter moorings, deployed over and near the seamount summit in March 1992 (CD66), indicated the presence of a clockwise flow associated with GMT, with typical speeds of ca. 5 cm s^{-1} near the slope (*figure 2a*). At rig D, one result is clearly showing a southeast flow but this is a near surface record (58 m depth) where conditions will be more variable. The measurements were made between spring and neap tides or centred about 5 days after springs so measured semidiurnal currents and isotherms displacements would have been larger at spring tides. The current meter results

Table II. Tidal analysis and mean of short term current meter deployments and self-contained ADCP data.

		mean		M_2						Inertial/K_1					
	Depth (m)	cm s^{-1}	ºT	a (cm s^{-1})	b (cm s^{-1})	ϕ (ºg)	θ (ºT)	ε	ROT	a (cm s^{-1})	b (cm s^{-1})	ϕ (ºg)	θ (ºT)	ε	ROT
Rig A CM7401	50	2.9	119	13.9	10.5	327	089	0.75	C	2.1	1.4	150	136	0.66	C
Rig A CM7517	148	2.4	109	19.6	14.4	344	092	0.73	C	8.0	7.2	228	163	0.90	C
Rig B CM5204	222	1.7	105	11.7	10.1	002	088	0.86	C	23.7	17.6	126	012	0.74	C
Rig B CM1260	423	6.9	139	22.6	9.1	314	042	0.40	C	7.2	0.1	245	048	0.01	A
Rig C CM421	28	5.8	326	30.4	22.2	285	051	0.73	C	5.8	2.6	178	128	0.44	C
Rig D CM8010	58	12.4	112	17.9	10.8	277	027	0.61	C	5.4	2.6	179	157	0.49	C
Rig D CM6372	259	2.9	314	12.9	6.7	291	022	0.52	C	14.5	3.7	260	130	0.25	C
Rig D CM7943	530	3.3	267	8.7	1.5	226	006	0.18	A	2.3	0.7	188	008	0.32	C
Rig L ADCP															
BINS 01-08	288	1.6	211	13.2	8.4	358	088	0.64	C	12.2	7.9	118	042	0.65	C
BINS 09-16	256	2.3	089	16.5	11.0	352	084	0.67	C	17.5	14.8	89	016	0.85	C
BINS 17-24	224	3.6	098	17.6	9.4	334	076	0.53	C	15.4	13.7	229	155	0.89	C
BINS 25-32	192	3.6	109	18.4	9.6	336	088	0.52	C	8.2	6.0	217	135	0.73	C
BINS 33-40	160	3.2	101	18.6	12.5	327	087	0.67	C	3.5	1.7	286	128	0.47	C
BINS 41-48	128	4.0	102	18.5	15.1	294	060	0.82	C	4.0	3.1	225	010	0.79	C

a is semi-major axis, b is semi-minor axis, ϕ is phase, θ is orientation, $\varepsilon = b / a$ ratio and ROT is sense of rotation of the current ellipse.

show the presence of semidiurnal M_2, inertial and diurnal tidal K_1 currents (*table II*). Although the records are short, the analysis for M_2 will be fairly reliable for the observation period as the analysis was derived with related S_2 and N_2 constituents (Schwiderski, 1981a), for example, for S_2 elevation values in the GMT region). However, at the latitude of 30°N, the inertial period f and K_1 diurnal period are indistinguishable for short records. Standard tidal analysis procedures fail and it is incorrect to relate K_1 with O_1 (Schwiderski, 1981b), for example, for O_1 elevation values in the GMT region). It is most probable that the large diurnal signal 24 cm s^{-1} at rig B is due to internal inertial motions associated with the abrupt topography of the bank. Similar large diurnal/inertial values (19 cm s^{-1}) were found at rig L in the ADCP data. Meincke (1971) found K_1 speeds of 6 cm s^{-1} on the Tablemount but did not report the presence of a much larger (25 cm s^{-1}) diurnal inertial signal. A least-squares analysis showed maximum diurnal energy levels in a slightly subinertial frequency band (period 24.3 h).

The effectively continuous ADCP data (4 m bins vertically) near the bank centre show that although the diurnal currents can dominate at 240 m depth, semidiurnal motions are generally larger. Large semidiurnal currents were found near the surface (M_2 semi-major axis 30 cm s^{-1}, 28 m depth, rig C, *table II*) and near the sea floor (23 cm s^{-1}, rig B, 423 m depth). The semidiurnal motion is partly internal as can be seen in the phase change (and direction change) with depth. *Table II* shows a change of 64° in 160 m, with an advance of phase at shallower depths, perhaps suggestive of upward propagating internal tidal energy from the upper slopes of GMT where the slope gradient becomes critical.

The diurnal motion at rig L also shows a short vertical wavelength structure in the ADCP beam centred near 240 m depth with a phase change (but also largely compensated by orientation) of about 100° in passing from 20 m off bottom to 120 m off bottom. These results might represent inertial energy propagating upward from the sea floor of the Tablemount. We note that the motion is rotary clockwise as expected. The clockwise diurnal motion can be seen in the buoy tracks (drogues at 200 m) on and around GMT also at the 5 km scale (or semi-major current ellipse 20 cm s^{-1}).

The temperature is also measured at the mooring with a calibrated value at each current meter every five minutes. The ADCP also records a bottom temperature. The mean values over a common 2 day period, from yearday 68.25 to yearday 70.25 (1992), are given in *table I, column 8*. These values can be important in establishing whether the near synoptic distribution of isotherms obtained from XBT/CTDs is a transient pattern or an internal motion or represents a more permanent feature. The mean tempera-

ture values are also a climate reference for future visits to GMT during the same late winter period but in different years.

3.2. Thermohaline structure, chlorophyll *a* and primary production

In March 1992, the upper water column over GMT was colder and fresher than in the surrounding waters (*figure 3*), giving a domelike temperature structure in the upper layer. Small scale inversions of temperature were found but these were compensated for density by salinity and were therefore stable. These structures indicate that some mixing occurs by interleaving of water. The 19.3ºC isotherm ascended from 150 m outside seamount up to the surface on the seamount summit (depth < 350 m). A similar domelike structure was observed in salinity with the 36.8 isohaline rising from 150 m depth up to the surface.

Bottom mixing was clearly evident with near bottom homogeneous layers of 30 m vertical extent. The central station CTD 15 was warmer nearer the bottom than the surrounding water at the same depth, causing the isotherms to tilt downwards near the sea floor on top of the bank. This overall effect could result in a weak vertical circulation with cooler water moving inwards along the sea floor and then slowly rising over the more central region of the bank.

Depression of isotherms was observed at CTDs 20 and 21, corresponding to the seamount slope (depth 350–3000 m) and CTD 19 corresponding to deep-sea waters (depth > 3000 m); this effect occurred on the eastern side of the seamount and might reflect a southward flow on the eastern flank. Oxygen concentrations were 5.3 mL L^{-1} in the mixed layer and fell to 4.7 mL L^{-1} near the sea floor on the GMT summit, similar to the values given for 30°N in Pingree (1997). Associated with the outcropping isotherms, a clear biological response was detected on the seamount slopes and summit (*figure 4*). Relatively higher chlorophyll *a* concentrations, > 0.15 mg m^{-3} were measured at stations 11 and 16 located over the slope and GMT summit respectively. A deep chlorophyll maximum was not detected. Underway surface fluorescence measurements carried out along a series of sections crossing the GMT also showed this slope related distribution of chlorophyll *a*. However, primary production rates in the upper 20 m above the seamount centre were higher than over slope waters (> 0.4 mgC m^{-3} h^{-1}). Carbon incorporation rates decreased sharply below 25 m.

In December 1993 (cruise CD 83), three stations located over GMT, on the slope and in deep-sea waters were visited. The upper mixed layer extended down to 100 m depth, except at slope waters where it was slightly shallower (ca. 80 m). The vertical thermal distribution showed the eroding seasonal thermocline with temperature decreasing from 20.5ºC at 100 m to 18.5ºC at 120 m. Salinity profiles show a similar pattern with values increasing from 36.5 at 120 m depth to 37.0 at 100 m, except at the slope station. NO_3 concentrations were low in the upper 80 m of the water column (< 0.05 µM, (Pingree et al., 1999). Significant increases in nitrate were first found at 150 m depth (~1 µM) but nitrate increased progressively with depth reaching values of 3 µM at 200 m and 6 µM near the sea floor at 265 m. Oxygen concentrations (CD83, profiles not shown) also matched the thermocline with surface values of about 5.0 mL L^{-1} in the mixed layer and falling to 4.7 mL L^{-1} near the sea floor on the GMT summit. Chlorophyll *a* concentrations exceeded 0.2 mg m^{-3} in the upper 80 m, with vertical distribution related to the pycnocline. Although surface chlorophyll *a* concentration was only just higher over the slope, depth-integrated total chlorophyll *a* was higher over GMT (30 mg m^{-2}) than in deeper waters (23–24 mg m^{-2}). The contribution of cells larger than 2 µm to total chlorophyll *a* was slightly higher over GMT (10.4%) than over slope (7.0%) and in deep-sea waters (5.7%).

Maximum primary production rates were higher at deep-sea station (0.8 mgC m^{-3} h^{-1} at 20 m depth) than over GMT (< 0.6 mgC m^{-3} h^{-1} at 60 m depth). Depth-integrated primary production rates were 44 mgC m^{-2} h^{-1} over GMT and 58 mgC m^{-2} h^{-1} in deep-sea waters. Cells larger than 2 µm accounted for 20.3% and 22.7% of total primary production over GMT and in deep-sea waters respectively, so significant differences in the relative contribution of phytoplankton size-fractions to total primary production were not detected.

In April 1999, seven stations were occupied in the GMT region as part of Azores II cruise. Outcropping of isotherms or isohalines did not occur over the seamount summit with the development of stratification in the upper 50 m of the water column, though small scale stable salinity compensated temperature inversions were

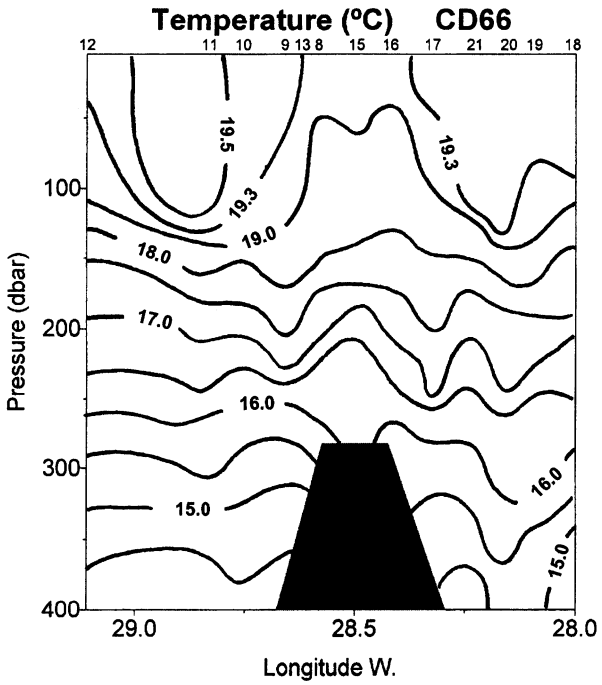

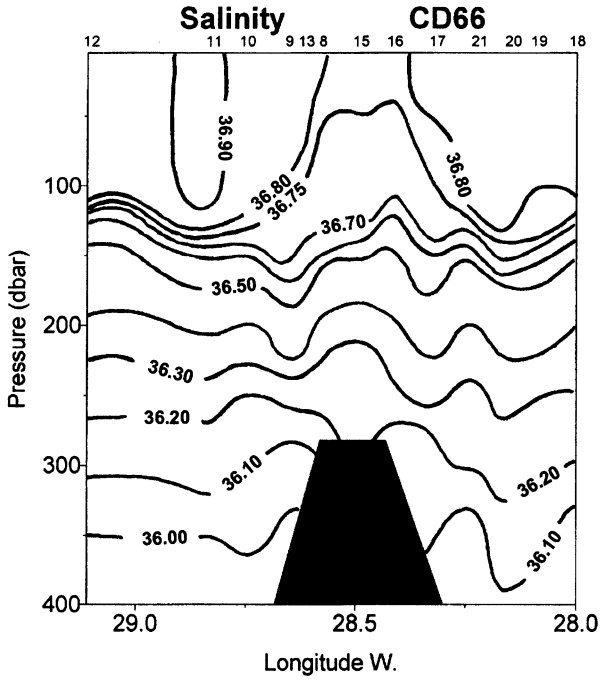

Figure 3. Vertical sections of temperature and salinity across GMT in March 1992 (CD 66), showing cooler (fresher) surface water, and warm (saltier) mixed water near the sea floor.

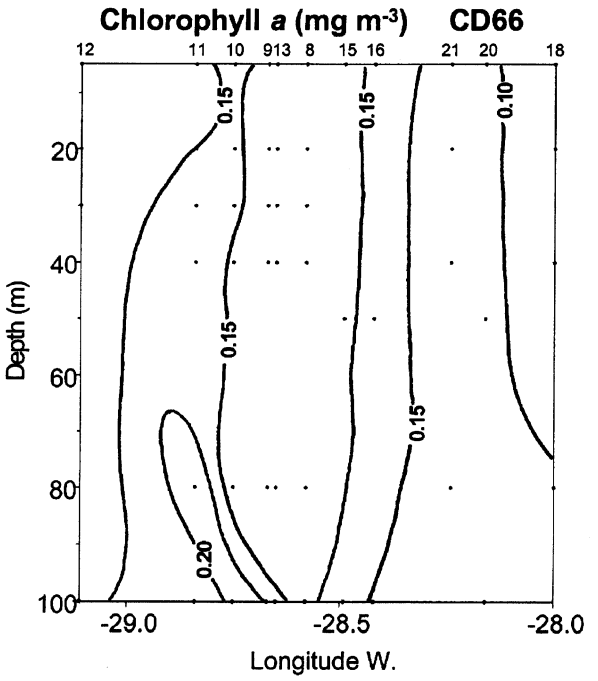

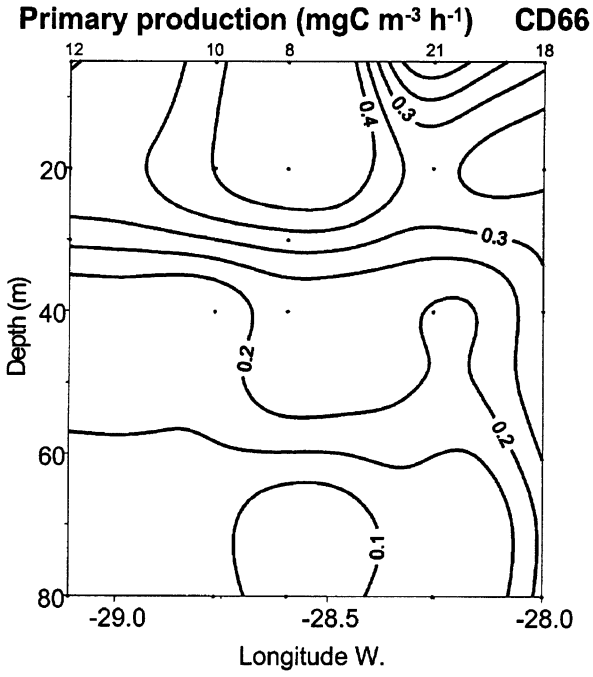

Figure 4. Vertical distribution of chlorophyll *a* and primary production across GMT in March 1992 (CD66) in the upper 100 m.

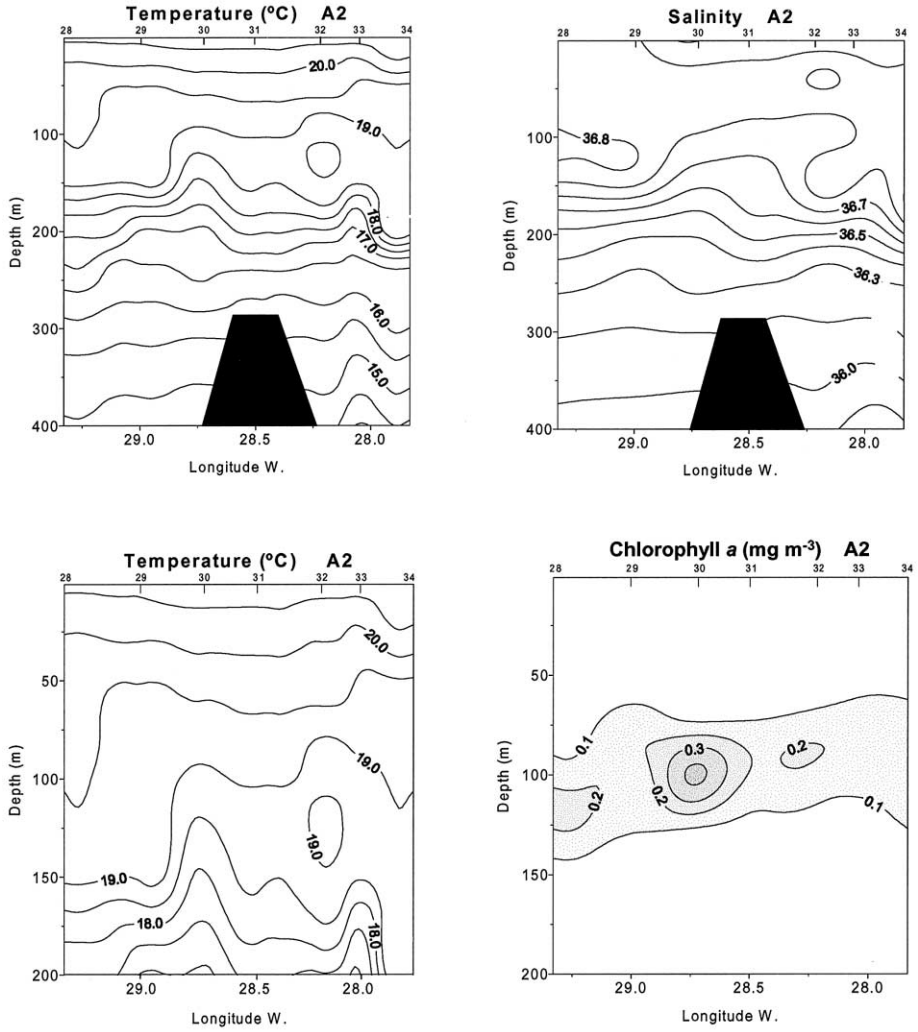

Figure 5. Vertical distribution of temperature and salinity in the upper 400 m, and temperature and chlorophyll *a* in the upper 200 m across GMT in April 1999 (Azores II).

evident (*figure 5*). Maximum chlorophyll *a* values (> 0.3 mg m^{-3}) were observed at 100 m depth associated with a shallower thermocline over the seamount slope (station 30). In contrast to March 1992, enhanced surface chlorophyll *a* levels were not detected. The highest depth integrated chlorophyll *a* concentration was measured in slope waters (14 ± 2 mg m^{-2}) but this value was not significantly higher ($P > 0.05$) than values calculated for GMT (11.6 ± 0.4 mg m^{-2}) and deep-sea waters (13.4 ± 0.4 mg m^{-2}). The contribution of cells larger than 2 µm to total chlorophyll *a* was lower than 40% in all the sampled stations, except at station 30 (> 65%), where relatively higher chlorophyll *a* concentrations were measured.

Rates of carbon incorporation by phytoplankton were measured at three stations located over GMT (station 31), slope (station 32) and deep-sea waters (station 34). Depth-integrated total primary production was higher over GMT (19 mgC m^{-2} h^{-1}) as compared to slope (12 mgC m^{-3} h^{-1}) or deep-sea waters (13 mgC m^{-2} h^{-1}). Primary production maxima were progressively shal-

Table III. Average depth-integrated chlorophyll *a* and primary production rates.

	Integrated chlorophyll *a*			Integrated primary production		
	depth (m)	mg m^{-2}	*n*	depth (m)	mgC m^{-2} h^{-1}	*n*
GMT (< 350 m depth)						
March 1992 (CD 66)	150	15 ± 1	6	100	23	1
December 1993 (CD 83)	150	30	1	120	44	1
October 1995 (CD 97)	150	23	1			
August 1998 (Azores I)	150	46	1	130	36	1
April 1999 (Azores II)	150	11.6 ± 0.4	5	150	19	1
Slope (350–3000 m depth)						
March 1992 (CD 66)	150	18 ± 3	4	100	19 ± 1	2
December 1993 (CD 83)	150	23	1	120	54	1
April 1999 (Azores II)	150	14 ± 2	2	150	12	1
Deep-sea waters (> 3000 m depth)						
March 1992 (CD 66)	150	12 ± 4	2	100	23 ± 3	2
December 1993 (CD 83)	150	24	1	120	58	1
October 1995 (CD 97)	150	23	1			
April 1999 (Azores II)	150	13.4 ± 0.4	4	150	13	1

Rates (± SEE) were calculated in March 1992 (CD66), december 1993 (CD83), october 1995 (CD 97), august 1998 (Azores i) and april 1999 (Azores ii) over the GMT, slope and deep-sea waters; *n* represents number of stations.

lower at stations located away from the GMT summit. Cells larger than 2 µm contributed to a slightly higher proportion of total production at slope (50.3%) than at deep-sea waters (46.4%) or over GMT (36.2%).

Depth-integrated phytoplankton biomass and primary production rates averaged for all the stations sampled during the five cruises generally did not show significant differences among stations located over GMT, slope or deep-sea waters (*table III*) though seasonality was evident. The depth-integrated chlorophyll *a* concentration was higher over GMT in December 1993 (30 mg m^{-2}), whereas in March 1992 and April 1999, a slightly higher integrated phytoplankton biomass was measured at the deeper stations. A consistent onshelf–offshelf gradient in depth integrated primary production rates was not observed. Higher depth-integrated carbon incorporation rates were recorded over the seamount summit in April 1999, the opposite trend was found in December 1992.

3.3. Phytoplankton composition

Marked differences between waters associated with the seamount and off-shelf waters were also detected in the relative contribution of various taxonomic groups to total microplankton biomass (*figure 6*). Total microplankton carbon biomass in March 1992, showed higher values at slope stations, in agreement with the distribution of chlorophyll *a* described above (*figure 4*). Small flagellates were the dominant group in terms of biomass with maximum values of 5.3 mgC m^{-3} over the slope. A similar distribution pattern was observed for dinoflagellates, coccolithophores and micrograzers. Diatom biomass was significantly higher at the central region of GMT, with values exceeding 0.65 mgC m^{-3}, whereas it was negligible at slope and deep-sea waters. The most abundant diatom species were *Guinardia flaccida*, *Leptocylindrus danicus*, *Bacteriastrum delicatulum* and several species of the genus *Chaetoceros*. Changes in microplankton biomass distribution were also reflected in variations in the biochemical composition of particulate organic matter. Depth averaged protein/carbohydrate ratios were lower at the seamount summit (< 1) than in the rest of the seamount area (> 1.25).

In December 1993, total depth-integrated microplankton carbon biomass, as well as integrated chlorophyll *a* was higher over GMT. Small flagellates were also the dominant group showing maximum values of 5.6 mgC m^{-3}. The diatom biomass was only slightly higher over the seamount (cf. March 92) with values always lower than 0.1 mgC m^{-3}. *Leptocylindrus mediterranea* and *Nitzschia delicatissima* were the most abundant diatom species.

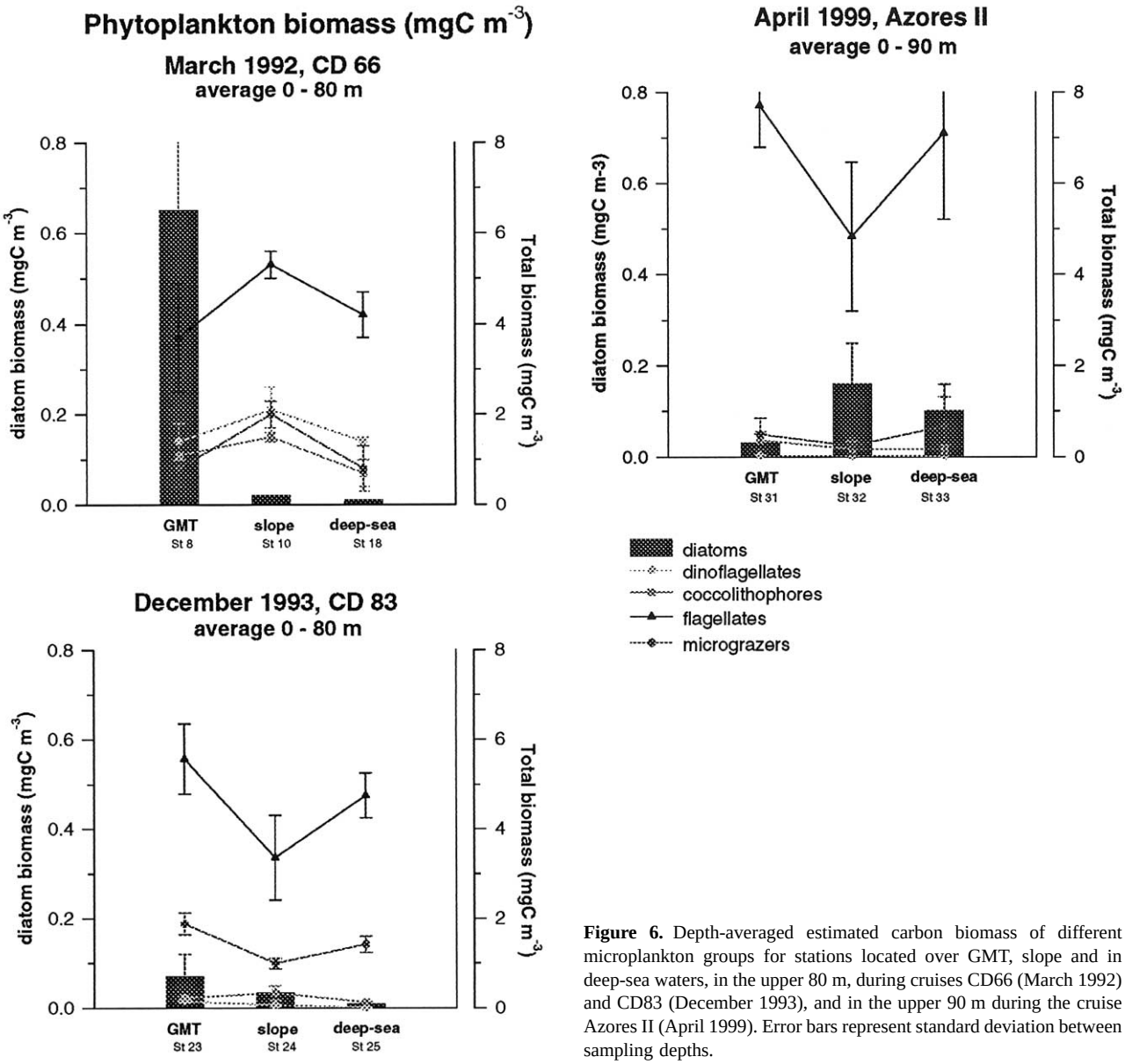

Figure 6. Depth-averaged estimated carbon biomass of different microplankton groups for stations located over GMT, slope and in deep-sea waters, in the upper 80 m, during cruises CD66 (March 1992) and CD83 (December 1993), and in the upper 90 m during the cruise Azores II (April 1999). Error bars represent standard deviation between sampling depths.

In April 1999, total depth-integrated microplankton carbon biomass was both relatively high over GMT and in deep-sea waters. The phytoplankton composition was not studied at station 30 (water depth 1305 m, i.e. slope waters), where the maximum integrated chlorophyll *a* values was found (*figure 5*). As occurred on the other two cruises, small flagellates were dominant group, with values higher than 7 mgC m^{-3} over GMT and deep-sea waters. Diatom biomass showed slightly higher values at slope waters (0.16 mgC m^{-3}), species of the genus *Rhizosolenia* being the most abundant.

3.4. Seasonal and short-term temporal variability over Great Meteor Tablemount

Seasonal changes of physical variables, phytoplankton biomass and primary production rates over Great Meteor

Tablemount were studied by gathering the data obtained from all the cruises (*figure 7*). In March 1992, the mixed layer depth extended down to 150 m, then gradually became shallower reaching 50 m depth with summer seasonal thermal and haline stratification. The chlorophyll *a* and primary production maxima were found at deeper depths. Although the upper water column was relatively mixed in April 1999, chlorophyll *a* and primary production maxima were located at subsurface depths (100 m). Relatively high values of phytoplankton biomass (0.7 mg m^{-3} chl *a*) and production (0.6 mgC m^{-3} h^{-1}) were measured at 100 m in August. In October (CD97) at the end of the heating season, the fluorescence maximum (0.3 mg m^{-3} chl *a*) was at 105 m (CTDs 11,12 and 13) just below the seasonal thermocline. The corresponding oxygen concentration maximum was 5.5 mL L^{-1} at 80 m depth with surface and bottom values (306 m depth) of 4.7 mL L^{-1}. This excess oxygen (0.3 mL L^{-1}) at depth (cf. March, 5.2 mL L^{-1} at 80 m) represents the cumulative effects of photosynthesis over respiration during the productive season (March to October). Although nitrate (NO_3) values were low at the surface (0.08 µM) significant increases occurred at 120 m (0.3 µM NO_3) with values of 4.5 µM at 200 m and 6.9 µM at 300 m near the sea floor, similar to December (CD83) values.

The pattern of seasonal variability in mixed layer depth and degree of stratification translates into 2–3 fold changes in depth-integrated chlorophyll *a* and primary production rates. The highest integrated primary production and chlorophyll *a* values were measured in December 1993 (44 mgC m^{-2} h^{-1}) and August 1998 (46 mg m^{-2}), whereas the lowest values were both measured in April 1999 (19 mgC m^{-2} h^{-1} and 11.6 ± 0.4 mg m^{-2}). On average (using all the data in the vicinity of seamount), depth-integrated phytoplankton biomass and primary production rates decreased in the period December to April.

Changes in the physical and biological characteristics of GMT also occurred at shorter temporal scales. The data set derived from four short-term current meter moorings and one self contained ADCP on GMT in March 1992 displayed temperature and speed variations showing distinct semidiurnal and diurnal/inertial periods. Temperature variations of more than 2ºC over a 12 h period were monitored at rig B at a fixed depth (423 m) (*figure 8*). These changes would translate into vertical excursions of isotherms of 170 m (*figure 9*). Semidiurnal currents are conspicuous with a semi-major axis of 23 cm s^{-1} but maximum speeds reached 46 cm s^{-1} over the 4 days measurement period at this position. At mid depths (222 m) on the same rig, the currents were essentially diurnal due to the presence of inertial motion with a semi-major axis of nearly 24 cm s^{-1} (*figure 10*). Maximum speeds reached 52 cm s^{-1} at this level (222 m). The diurnal current energy with speeds reaching 24 cm s^{-1} was concentrated into a band about 70 m thick (half energy levels) centred near 232 m depth (*figure 9*). The vertical shear was greatest near the diurnal/inertial beam where the mean gradient Richardson number based on diurnal current and mean temperature will be at a minimum. The gradient Richardson number is of order 1 near 200 m and internal mixing is most likely at this level over the Tablemount summit. Progressive vector diagrams showed that the diurnal motion in the inertial beam at rig L (with maximum levels ~18 cm s^{-1} at 240 m) and the diurnal motion at rig B (where the inertial signal reached 24 cm s^{-1} at 222 m depth) were coherent, suggesting a fairly spatially uniform circular clockwise rotary motion over the Tablemount summit. Temperature variations of 1.6°C at 222 m would correspond to isotherm displacements of 100 m. The temperature signal at 222 m (*figure 10*) is less coherent than at 423 m (*figure 8*).

Short-term variations in temperature, salinity and chlorophyll *a* were also studied over GMT (30°N, 28.5°W) in April 1999 (Azores II cruise) with five CTD casts conducted over an 8 h period. The 18ºC isotherm and the 36.4 isohaline ascended more than 40 m over a 2 h period. The chlorophyll *a* maximum (> 0.1 mg m^{-3} values), which was located in the pycnocline (*figure 11*), showed the same vertical displacements.

Mean temperature (and salinity) profiles in March (1992) showed that the internal ray characteristic, $c = 0.03$, for semidiurnal internal motions could match the upper slope gradient, *s*, of GMT near the 400 m depth contour with $s = c = 0.03$, particularly along the eastern flank. The value of *c* did not vary markedly with season, as below a 120 m depth temperature (density) seasonal changes with depth were not significant (*figure 7*). Although, we have not demonstrated a 'little splash' region (or a focus with marked internal wave activity and mixing) near the bank centre (Pingree and New, 1995), the theoretical result depicting a central region receiving internal energy from all directions is consistent with the marked internal tide activity found both on and off the bank. The drogued thermistor chain (moving with the

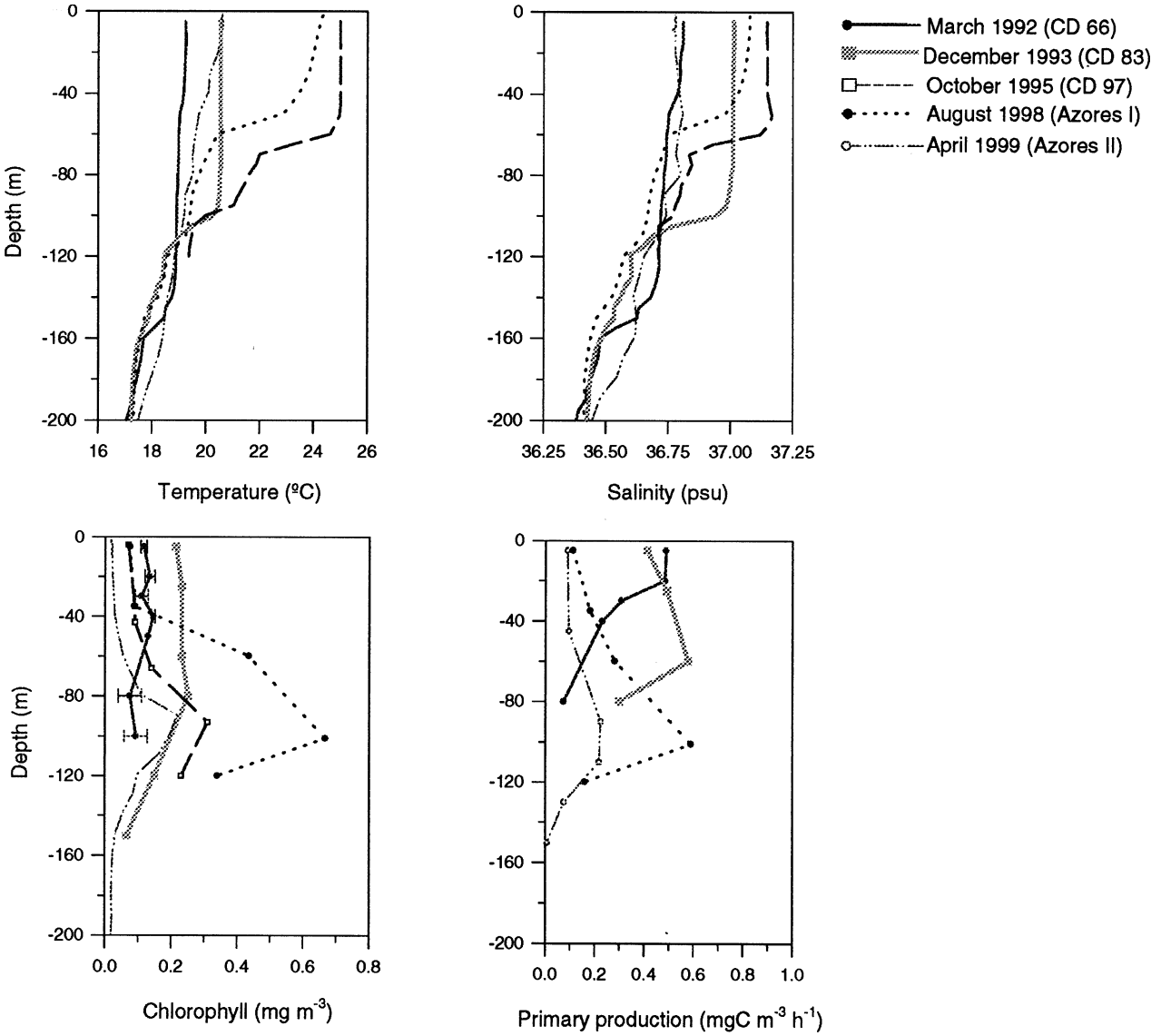

Figure 7. Vertical profiles of temperature, salinity, chlorophyll *a* and primary production in March 1992 (CD66), December 1993 (CD83), October 1995 (CD 97), August 1998 (Azores I) and April 1999 (Azores II) over the GMT summit. Error bars represent standard error between different stations visited during the same cruise.

tidal flow near the bank centre, see methods) showed semidiurnal internal tidal motion and internal waves of short period with peak to trough amplitudes of typically 80 m in the 100 m to 200 m depth range. The maximum internal displacement was about 150 m or from 60 m to 210 m depth. We note, as is well known, that the diurnal/inertial currents, although of large internal amplitude (*table II, figure 9*) are not associated with the same relative isotherm displacement as semidiurnal currents (for example, *figure 9*). In summary, the bank centre will receive internal energy from all round the shelf-break region (400 m). In addition to mixing by internal waves, there will be bottom mixing on the summit of GMT itself and mixing by diurnal shear 100 m above the summit. This mixing will result in heat flowing downwards (in all seasons below the mixed layer) and the warmed water at the sea floor will be replaced by cooler denser water (e.g. estuarine circulation). This will result in a slow upward

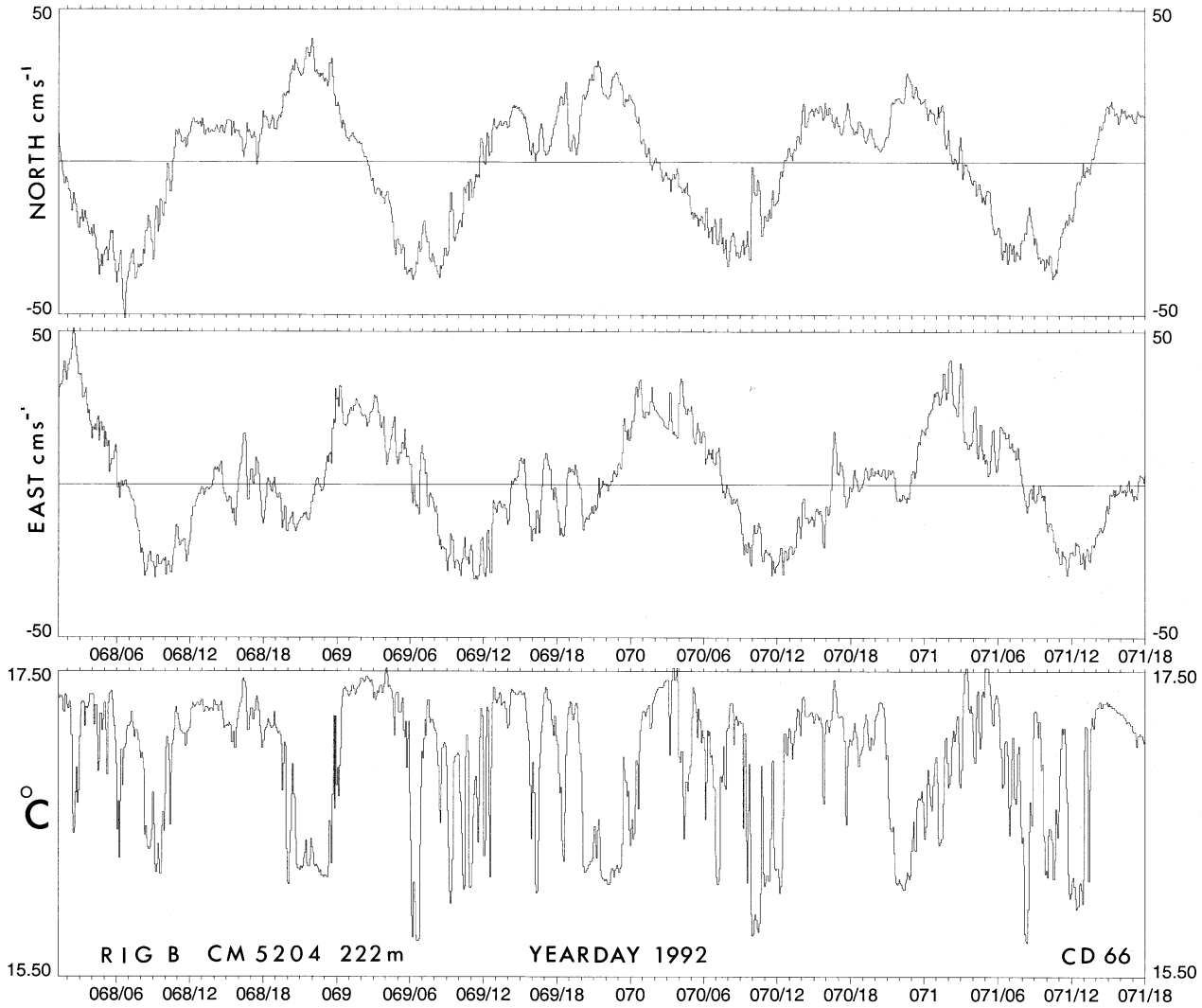

Figure 8. Short-term variations of temperature and north and east component of velocity against yearday 1992 showing dominant semidiurnal motion obtained from current meter 1260 located near the sea floor at 423 m depth (on rig B, water depth 435 m) in March 1992 (CD 66).

vertical motion that may result in anticyclonic motion (Meincke, 1971) and a cooling of the sea surface over the summit as was apparent on the 30°N section in March 1992 (*figure 3*).

4. DISCUSSION

Several observational (Angel and Fasham, 1983; Falkowski et al., 1991; Siegel et al., 1999) and modelling studies (McGillicuddy and Robinson, 1997; McGillicuddy et al., 1995; Oschlies and Garçon, 1998), indicate that mesoscale features could play an important role in nutrient supply to the upper productive layer in subtropical nutrient depleted regions.

Among the considerable diversity of mesoscale features, seamounts have been reported as highly dynamic areas from both the physical and biological perspective. Several studies have demonstrated uplifting of isotherms (Meincke, 1971; Owens and Hogg, 1980; Roden, 1991; Vastano and Warren, 1976) and chlorophyll and primary production enhancement linked to these physical singularities (Rogers, 1994). Lophukin (1986) reported en-

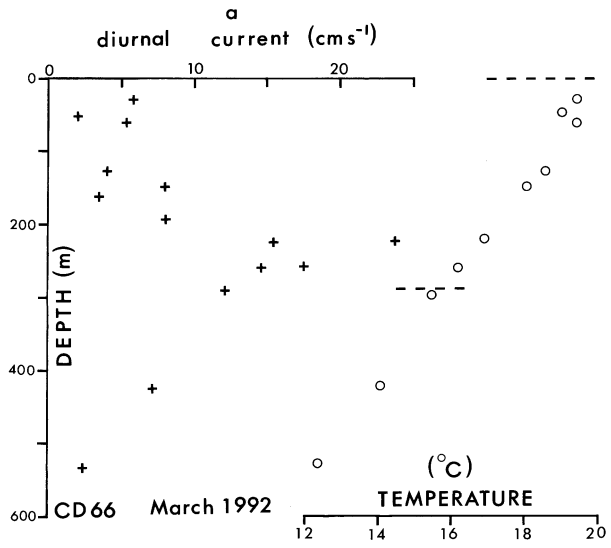

Figure 9. Vertical distribution of diurnal inertial currents (*a* semi-major axis) and mean temperatures obtained from the mooring rigs deployed on GMT (CD66, see *tables I and II*)**. Dashed lines denote the surface and the depth of rig C (288 m) on the shallowest part within the main 300 m contour of the mount summit.**

hanced ATP concentrations associated with waters over the slopes of different Atlantic seamounts, and Dower et al. (1992) detected low light transmission values above Cobb seamount in the North East Pacific. Similar results were reported by Odate and Furuya (1998) at Komahashi No. 2 Seamount. The shallowing and intensification of the subsurface chlorophyll *a* maximum, as well as increases in diatom biovolume and in the production to biomass ratios have been also detected at Cobb Seamount (Comeau et al., 1995).

As already mentioned in the introduction, previous studies carried out on seamounts did not show a consensus on the effect of these topographic features on phytoplankton production and/or biomass. In this connection, the results presented in this paper failed to demonstrate persistent increases of depth-integrated primary production and biomass over GMT. However, they show enhanced phytoplankton biomass and production rates related to vertical displacements of the upper pycnocline in March 1992, manifested by outcropping of isotherms and isohalines (CD66, *figures 3*, *4*). By April, biomass and production were already located in the thermocline (Azores II 1999, *figure 5*). Depth-integrated primary production rates measured over GMT (23 mgC m^{-2} h^{-1}) in March 1992 did not differ either from published values for a nearby region, 30.0º N – 26.0º W, during cruise CD66 (29 mgC m^{-2} h^{-1}; Fernández and Pingree, 1996) or from averaged carbon incorporation rates estimated using a data set sampled during three cruises carried out from September 1995 to October 1996 in the subtropical NE Atlantic, approximately along the 20ºW section (Marañón et al., 2000).

The biological effects of seamounts are also qualitatively manifested. It has been hypothesized that seamounts, due to their pattern of water motion, constitute a trapping mechanism whereby biological populations could remain partially isolated (Belyanina, 1984; Moiseyev, 1986). Therefore pelagic communities living over and around seamounts are likely to differ in terms of biomass and species composition if there is significant trapping of water. In this regard, we have estimated a mean residence time of the water over GMT as 21 days (see results), equivalent to a mean displacement velocity of 2.9 km-day^{-1}, a value considerably larger than the diffusive velocity scale 0.7 km day^{-1}. It is noted that the advective velocity scale is about two and a half times less than the mean displacement velocity estimated for the surrounding oceanic region, 7 km day^{-1}, and five times more than the radial diffusive speed estimated for STORMs (subtropical oceanic ring of magnitude) 0.5 km day^{-1} (in the upper layer < 500 m depth and within a radius of 100 km of the eddy centre; Pingree et al., 1999) travelling westward through the region just to the north. However, the existence of temporal variability in the mean residence time of the water over GMT cannot be ruled out.

Clear differences were detected in the relative contribution of various taxonomic groups to total microplankton biomass between GMT and nearby waters in March 1992 (*figure 6*). Large diatoms, typical of shallow coastal areas, such as *Guinardia flaccida, Leptocylindrus danicus, Bacteriastrum delicatulum* and species of the genus *Chaetoceros*, were more abundant at GMT. Meincke (1971) observed an anticyclonic vortex above GMT and proposed enhanced vertical mixing on the plateau due to vertical shear in tidal currents as a mechanism for the generation of the vortex. However, in March 1992, careful averaging of the isotherms over GMT over a two days period showed that the differences in isotherm (isopycnal) levels on the bank and in deeper water (CTDs 12 to 18) were only about 20 m rather than nearly 100 m (*figure 3*). Any anticyclonic vortex would have to lie below 200 m depth since the drogued buoys did not find one. In December 1993, small differences in phytoplank-

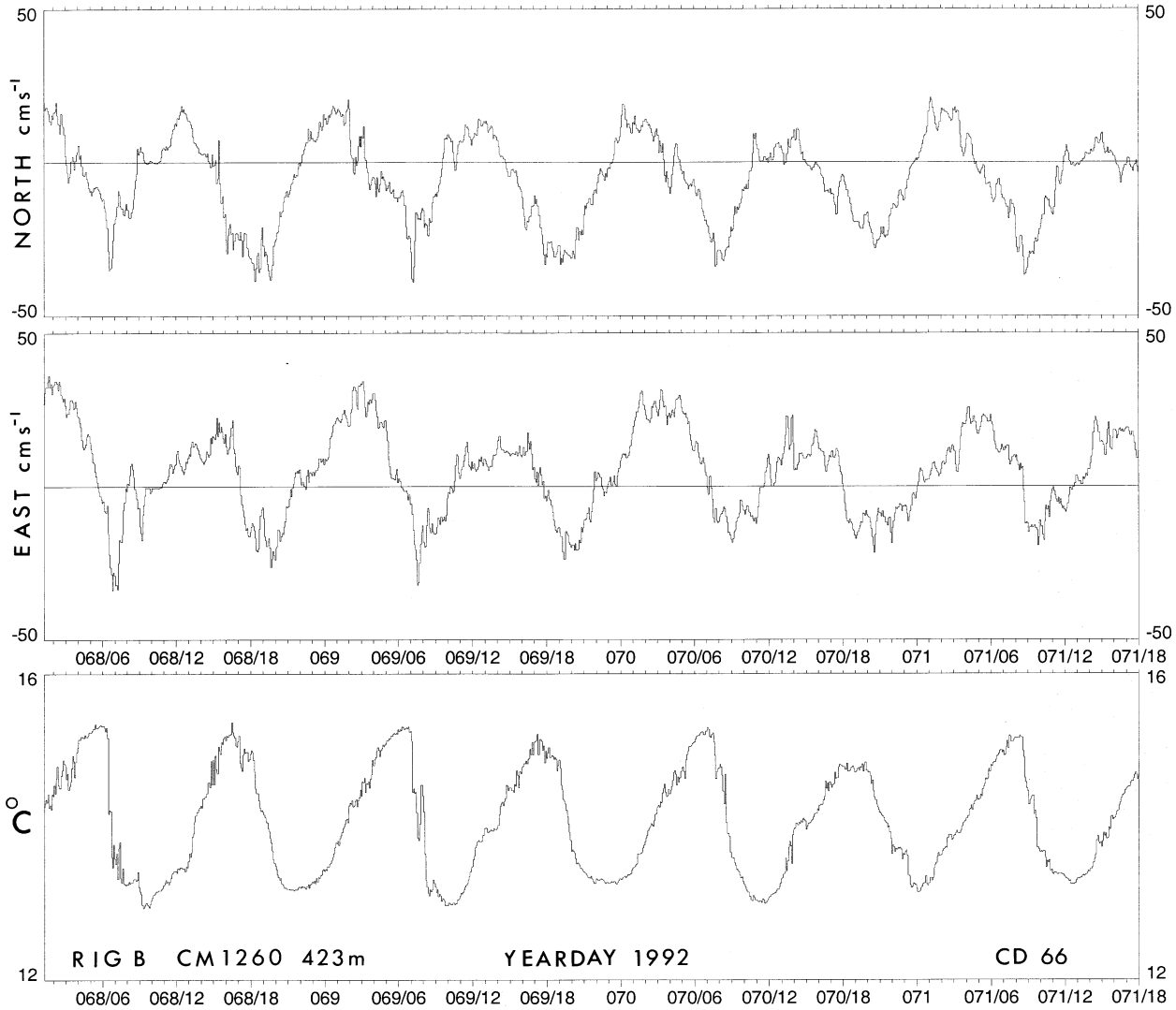

Figure 10. Short-term variations of temperature and north and east component of current against yearday 1992 showing dominant diurnal inertial motion obtained from current meter 5204 located at 222 m depth (on rig B, CD 66).

ton species composition between GMT and surrounding waters were also observed. However, no clear differences in phytoplankton composition were observed inside and outside GMT in April 1999 (Azores II). These results confirm the hypothesis that seamounts can constitute coastal-like habitats where phytoplankton species composition differ from the surrounding environment and therefore the pathway of carbon cycling through the planktonic food web is likely to became correspondingly altered (Legendre and Michaud, 1998).

To our knowledge, this is the first study focusing on the coupling between physical and biological components at seamounts over seasonal scales, however, the seasonal scale measurements were undersampled so that no conclusive results can be given. It should be borne in mind that the present study has been performed using data collected in five cruises carried out in different seasons throughout seven years and short-term physical variability may contribute to some of the longer period seasonal cycles. In order to tackle this problem it would be

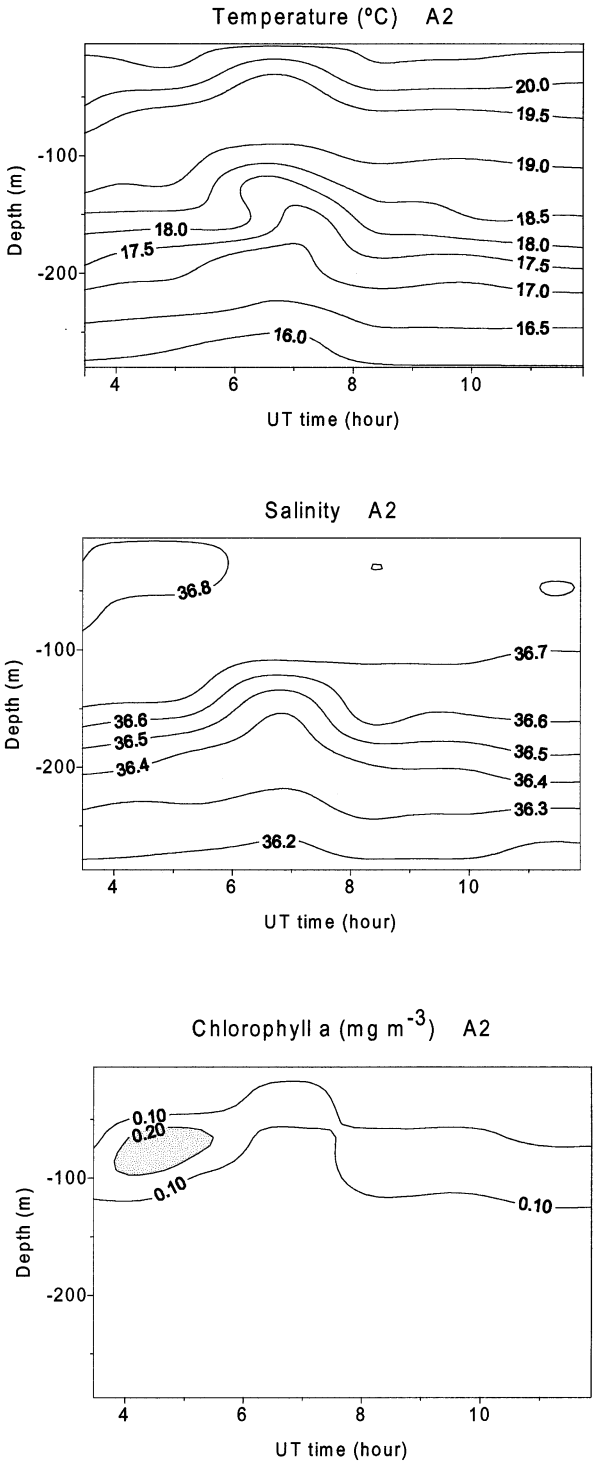

Figure 11. Short term variations of temperature, salinity and chlorophyll *a* measured on 26 April 1999 (Azores II) over GMT (30.0°N,28.5°W) (Station 31, 296 m depth; see *figure 5*.

necessary to measure all properties over a full semidiurnal or diurnal cycle in tidally dominant regions (see for example Pingree and New, 1995, reporting measurements made over several semidiurnal tidal cycles).

Short-term variability in the physical field could also account for the spatial mismatch observed in the distribution of primary production and chlorophyll *a* (e.g. *figure 4*), as a consequence of the different time-scales involved in the changes of phytoplankton standing stocks and rates of carbon incorporation. The uncoupling between primary production rates and chlorophyll *a* distribution observed in the CD66 cruise could also partially result from differential heterotrophic activity between GMT and surrounding waters. In this regard the ratio between the protein and chlorophyll *a* content of particulate organic matter was significantly higher ($P < 0.05$) over GMT (122.7) than outside seamount (77.7). This observation is consistent with a higher relative heterotrophic biomass over GMT, which could efficiently graze a portion of the newly synthesized biomass.

The analysis of records obtained from the different cruises for this study allows us to examine seasonality. The results showed that mixing and stratification of the water column are characterised by a distinct seasonal pattern, as shown by the gradual shallowing of the mixed layer as the seasonal thermocline becomes established during the summer. The stratification shows small changes below 100 m on the Tablemount. For example, in march 1992 (CD66), the temperature was 18.0°C at 150 m and 15.4°C on the bottom at 306 m depth (see *table I*), whereas in October 1995 (CD97) at the end of the heating cycle, the temperature at CTD 11 (30.0°N, 28.4°W) at 150 m was 18.9°C and 15.9°C at 308 m depth, 3 m above the bottom. Variations in measured mixed layer depth, from 60 to 160 m, are comparable with the 40–110 m reported for the region just south of the Subtropical Front outcrop (Pingree et al., 1999) and with the 20–130 m reported for North Atlantic Subtropical Gyre Province (Longhurst, 1998) and with the results obtained by Michaels et al. (1994) at the Bermuda Atlantic time-series study site in the Western Basin of the North Atlantic.

Sea true surface chlorophyll *a* concentrations and their temporal variability (*figure 7*), compare favourably with the seasonal cycle of surface chlorophyll *a* obtained from SeaWiFS monthly averaged data for the location (29.9°N, 28.4°W, with a 40×40 km average) of GMT (*figure 12*).

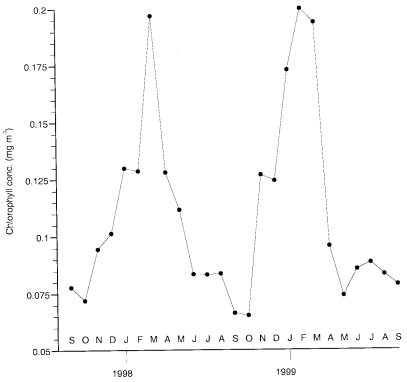

Figure 12. SeaWiFS seasonal cycles of chlorophyll *a* at GMT (28.4°W, 29.9°N) from September 1997 to September 1999. Mean monthly values shown (40 × 40 km average).

This seasonal cycle of surface chlorophyll *a* is also comparable to the SeaWiFS derived values given by Pingree et al. (1999) for subtropical seas or the region just south of the Subtropical Front in the Eastern Basin, so it does not seem that GMT has a distinct surface chlorophyll *a* signal with respect to the surrounding ocean though variations on shorter time scales can be related to the topography of the GMT region (e.g. March 1992). What is interesting in the SeaWiFS cycle (also sea true cycle) is that the values increase from about November to March, whereas in temperate seas the values do not increase steadily in the November to February winter period (see for example Garcia-Soto and Pingree, 1998). The GMT signal does differ slightly from the simple picture of a zonal northward movement of the spring bloom migration with the onset of seasonal stratification (Pingree et al., 1976). The proximity of GMT to the Madeira Rise, the Canary Islands and African upwelling region results in an influence from the east such that the GMT surface chlorophyll *a* signal in February and March is enhanced with respect to conditions to the west. To the west the surface subtropical chlorophyll *a* maximum is slightly weaker and occurs somewhat earlier, e.g. January/February. Finally we note that there is also variability in the monthly averaged SeaWiFS for the GMT region. In March 1998, there was a surface increase in chlorophyll *a* with respect to the surrounding oceanic region with values matching those to the north (300 km), whereas in March 1999, a clear GMT signal was not evident.

In addition to seasonal cycles of surface properties, we have measured subsurface changes in temperature, salinity, chlorophyll *a* and primary production over GMT and in the surrounding waters. These show the development of a subsurface chlorophyll *a* maximum in the seasonal thermocline and a primary production maximum at about 100 m depth. Vertically integrated or water column values of both the averaged chlorophyll *a* data and the averaged primary production values decreased in the December to April period. The corresponding mean production rate per unit of chlorophyll *a* also fell during this period.

The results presented in this paper clearly indicate that the relationship between the physical characteristics imposed by GMT and the response of phytoplankton populations is subjected to a high degree of temporal and spatial variability both at seasonal and shorter temporal scales. This may explain the difficulties to harmonise both independent observations made on different seamounts (Comeau et al., 1995; Dower et al., 1992; Lophukin, 1986; Odate and Furuya, 1998) and particular surveys of the same seamount (this study). New methodological approaches focused on the measurement of key variables at adequate time scales should be adopted in order to accurately quantify the biological effects of seamounts. Experiments carried out using moorings equipped with physical, optical and chemical sensors allowed a detailed description of the seasonal variability in the vertical distribution of chlorophyll *a* and photosynthetic rate for 240 days in the Sargasso Sea (Marra et al., 1992). A similar experimental approach might be developed in order to investigate the effects of seamounts on phytoplankton biomass and production.

We wish to thank RVS for support at sea and Ian Waddington (SOC) for deployment and recovery of the current meter moorings, and Dave Griffiths for data processing. Image processing of selected SeaWiFS data was kindly under taken by Dr Sam Lavender (PML, Remote Sensing Group). We thank Bob Head (PML) for the chlorophyll *a* determinations on CD66, CD83 and CD97 and Maria José Pazó and Eva Teira for the chlorophyll *a* and primary production determinations on Azores I and II. B. Mouriño was supported by a PFPI fellowship from the *Ministerio de Educación y Cultura* (Spain). This study was partially funded by the European Commission under the CANIGO contract MAS3CT960060.

REFERENCES

Angel, M.V., Fasham, M.J.R., 1983. Eddies and biological processes. In: Robinson, A.R. (Ed.), Eddies in marine science. Springer–Verlag, Berlin, pp. 493–524.

Belyanina, T.N., 1984. Observations on the ichthyofauna in the open waters of the Atlantic near the Great Meteor Seamount. J. Ichthyol. 24, 127–129.

Brink, K.H., 1990. On the generation of seamount-trapped waves. Deep-Sea Res. Part A 37, 1569–1582.

Codiga, D.L., 1997a. Physics and observational signatures of free, forced and frictional stratified seamount-trapped waves. J. Geophys. Res. 102, 23009–23024.

Codiga, D.L., 1997b. Trapped-wave modification and critical surface formation by mean flow at a seamount with application at Fieberling Guyot. J. Geophys. Res. 102, 23025–23039.

Codiga, D.L., Eriksen, C.C., 1997. Observations of low-frequency circulation and amplified subinertial tidal currents at Cobb Seamount. J. Geophys. Res. 102, 22993–23007.

Comeau, L.A., Vezina, A.F., Bourgeois, M., Juniper, K.S., 1995. Relationship between phytoplankton production and the physical structure of the water column near Cobb Seamount, Northeast Pacific. Deep-Sea Res. Part I 42, 993–1005.

Dower, J., Freeland, H., Juniper, K., 1992. A strong biological response to oceanic flow past Cobb Seamount. Deep-Sea Res. Part I 39, 1139–1145.

Eriksen, C.C., 1982. Observations of internal wave reflection off sloping bottoms. J. Geophys. Res. 87, 525–538.

Eriksen, C.C., 1985. Implications of ocean bottom reflection for internal wave spectra and mixing. J. Phys. Oceanogr. 15, 1145–1156.

Eriksen, C.C., 1991. Observations of amplified flows atop a large seamount. J. Geophys. Res. 96, 15.227–15.236.

Eriksen, C.C., Dahlen, J.M., Shillingford, J.T., 1982. An upper ocean moored current and density profiler applied to winter conditions near Bermuda. J. Geophys. Res. 87, 7879–7902.

Falkowski, P.G., Ziemann, D., Kolber, Z., Bienfang, P.K., 1991. Role of eddy pumping in enhancing primary production in the ocean. Nature 352, 55–58.

Fernández, E., Pingree, R.D., 1996. Coupling between physical and biological fields in the North Atlantic subtropical front southeast of the Azores. Deep-Sea Res. Part I 43, 1369–1393.

Garcia-Soto, C., Pingree, R.D., 1998. Late autumn distribution and seasonality of chlorophyll *a* at the shelf-break/slope region of the Armorican and Celtic Shelf. J. Mar. Biol. Ass. U.K 78, 17–33.

Genin, A., Boehlert, G.W., 1985. Dynamics of temperature and chlorophyll structures above a seamount: An oceanic experiment. J. Mar. Res. 43, 907–924.

Genin, A., Noble, M., Lonsdale, P.F., 1989. Tidal currents and anticyclonic motions on two North Pacific seamounts. Deep-Sea Res 36, 1803–1815.

Grasshoff, K., Ehrhardt, M., Kremling, K., 1983. Methods of seawater analysis. Verlag Chemie, Weinheim.

Holligan, P.M., Harris, R.P., Newell, R.C., Harbour, D.S., Head, R.N., Linley, E.A.S., Lucas, M.I., Tranter, P.R.G., Weekley, C.M., 1984. Vertical distribution and partitioning of organic carbon in mixed, frontal and stratified waters of the English Channel. Mar. Ecol. Prog. Ser. 14, 111–127.

Kaneko, A., Honji, H., Kawatate, K., Mizuna, S., Masuda, A., Miita, T., 1986. A note on internal wavetrains and the associated undulation of the sea surface observed upstream of seamounts. J. Oceanogr. Soc., Japan 42, 75–82.

Kunze, J.M., Toole, J.M., 1997. Tidally driven vorticity, diurnal shear, and turbulence atop Fieberling Seamount. J. Phys. Oceanogr. 27, 2663–2693.

Legendre, L., Michaud, J., 1998. Flux of biogenic carbon in oceans: size-dependent regulation by pelagic food webs. Mar. Ecol. Progr. Ser. 164, 1–11.

Longhurst, A., 1998. Ecological geography of the sea. Academic Press, San Diego, CA.

Lophukin, A.S., 1986. Distribution of ATP concentration above the seamounts in the Atlantic Ocean. Oceanology 26, 361–365.

Lueck, R.G., Mudge, T.D., 1997. Topographycally induced mixing around a shallow seamount. Science 276, 1831–1833.

Marra, J., Dickey, T., Chamberlin, W.S., Ho, C., Granata, T., Kiefer, D.A., Langdon, C., Smith, R., Baker, K., Bidigare, R., Hamilton, M., 1992. Estimation of seasonal primary production from moored optical sensors in the Sargasso Sea. J. Geophys. Res. 97, 7399–7412.

Marañón, E., Holligan, P.M., Varela, M., Mouriño, B., Bale, A.J., 2000. Basin-scale variability of phytoplankton biomass, production and growth in the Atlantic Ocean. Deep-Sea Res. Part I 47, 825–857.

McGillicuddy, D.J., Robinson, A.R., 1997. Eddy-induced nutrient supply and new production in the Sargasso Sea. Deep-Sea Res. Part I 44, 1427–1450.

McGillicuddy, D.J., McCarthy, J.J., Robinson, A.R., 1995. Coupled physical and biological modeling of the spring bloom in the North Atlantic: i) model formulation and one dimensional bloom processes. Deep-Sea Res. Part I 42, 1313–1357.

Meincke, J., 1971. Observation of an anticyclonic vortex trapped above a seamount. J. Geophys. Res. 76, 7432–7440.

Michaels, A.F., Knap, A.H., Dow, R.L., Gundersen, K., Johnson, R.J., Sorensen, J., Close, A., Knauer, G.A., Lohrenz, S.E., Asper, V.A., Tuel, M., Bidigare, R., 1994. Seasonal patterns of ocean biogeochemistry at the U.S. JGOFS Bermuda Atlantic time-series study site. Deep-Sea Res. Part I 41, 1013–1038.

Moiseyev, Y.V., 1986. Distribution of protozoans near seamounts in the western Indian Ocean. Oceanology 26, 86–90.

Navatov, U.N., Ozmidov, R.V., 1988. A study of turbulence over underwater mounts in the Atlantic Ocean. Oceanology 28, 210–217.

Noble, M., Mullineaux, L.S., 1989. Internal tidal currents over the summit of Cross Seamount. Deep-Sea Res. 36, 1791–1802.

Odate, T., Furuya, K., 1998. Well-developed subsurface chlorophyll maximum near Komahashi No. 2 Seamount in the summer of 1991. Deep-Sea Res. Part I 45, 1595–1607.

Oschlies, A., Garçon, V., 1998. Eddy-induced enhancement of primary production in a model of the North Atlantic Ocean. Nature 394, 266–269.

Owens, W.B., Hogg, N.G., 1980. Oceanic observations of stratified Taylor columns near a bump. Deep-Sea Res. 27, 1029–1045.

Pelaez, J., McGowan, J.A., 1986. Phytoplankton pigment patterns in the California Current as determined by satellite. Limnol. Oceanogr. 31, 927–950.

Pingree, R.D., 1997. The eastern subtropical gyre (North Atlantic): flow rings recirculations structure and subduction. J. Mar. Biol. Ass. U.K. 77, 573–624.

Pingree, R.D., Maddock, L., 1985. Rotary currents and residual circulation around banks and islands. Deep-Sea Res. 32, 929–947.

Pingree, R.D., New, A.L., 1995. Structure, seasonal development and sunglint spatial coherence of the internal tide on the Celtic and Armorican shelves and in the Bay of Biscay. Deep-Sea Res. 42, 245–284.

Pingree, R.D., Holligan, P.M., Mardell, G.T., Head, R.N., 1976. The influence of physical stability on spring, summer and autumn phytoplankton blooms in the Celtic Sea. J. Mar. Biol. Ass. U.K 56, 845–873.

Pingree, R.D., Garcia-Soto, C., Sinha, B., 1999. Position and structure of the Subtropical/Azores Front region from combined Lagrangian and remote sensing (IR/altimeter/SeaWiFS) measurements. J. Mar. Biol. Ass. U.K. 79, 769–792.

Roden, G.I., 1991. Mesoscale flow and thermohaline structure around Fieberling seamount. J. Geophys. Res. 96, 16653–16672.

Roden, G.I., Taft, B.A., 1985. Effect of the Emperor seamount on the mesoscale thermohaline structure during the summer of. J. Geophys. Res. 90, 839–855.

Rogers, A.D., 1994. The biology of seamounts. Advanc. Mar. Biol. 30, 305–350.

Schwiderski E.W., 1981a. The semidiurnal principal solar tide (S_2). Global ocean tides, part III. Atlas of tidal charts and maps. Naval Surface Weapons Center, pp. 81–122.

Schwiderski, E.W., 1981b. The diurnal principal lunar tide (O_1). Global ocean tides, part V. Atlas of tidal charts and maps, Naval Surface Weapons Center, pp. 81–144.

Siegel, D.A., McGillicudy, D.J., Fields, E.A., 1999. Mesoscale eddies, satellite altimetry, and new production in the Sargasso Sea. J. Geophys. Res. 104, 13359–13379.

Uchida, R.N., Tagami, D.T., 1984. Groundfish fisheries and research in the vicinity of seamounts in the North Pacific Ocean. Mar. Fish. Rev. 46, 1–17.

Vastano, A.C., Warren, B.A., 1976. Perturbations of the Gulf Stream by Atlantic II Seamount. Deep-Sea Res. 23, 681–694.

Vastano, A.C., Hagan, D.E., McNally, G.J., 1985. Lagrangian observations of surface circulation at the Emperor seamount chain. J. Geophys. Res. 90, 3325–3331.